Supporting Information

$CaSnO_3$ nanorods decorated Bi_2WO_6 nanosheets as a stable heterojunction photocatalyst for improved Photocatalysis and Nitrite sensing

Rakesh GN[a], Udayabhanu[a,b]*, Priyadarshini HN[a], Fahd Alharethy[c], Pavitra V[d], Anusha B R[a], Appu S[a], Aarti D P[e], Srinivas Reddy G[f], Nagaraju G[d], Prashantha K[a]*

[a]Centre for Research & Innovations, BGSIT, Adichunchanagiri University, B.G. Nagara, Mandya District, Karnataka 571448, India.
[b]Department of Chemistry, BMS Institute of Technology and Management, Yelahanka, Bangalore 560064, Karnataka, India.
[c]Department of Chemistry, College of Science, King Saud University, Riyadh-11451, Kingdom of Saudi Arabia.
[d]Energy Materials Research Laboratory, Dept. of Chemistry, Siddaganga Institute of Technology, Tumakuru, 572103, India.
[e]Department of Chemistry, School of Applied Sciences, REVA University, Bangalore, 560064, India
[f]Department of Physics and Chemistry, Mahatma Gandhi Institute of Technology, Hyderabad, Telangana -500075
Corresponding authors*: udayabhanubc@gmail.com & prashantha.k@gmail.com*

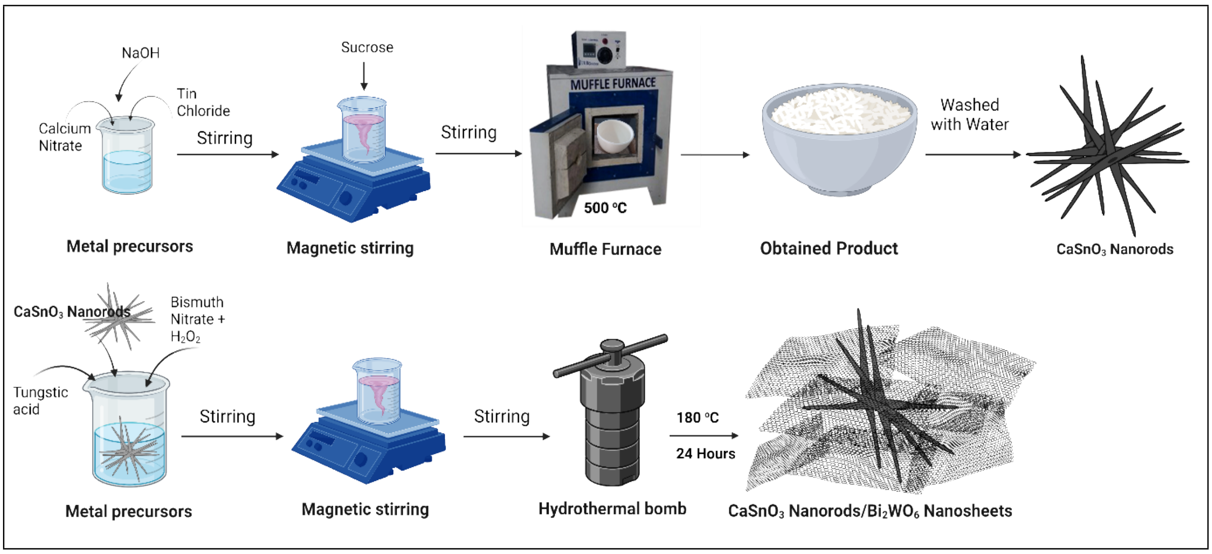

Fig. S1. Schematic representation for the synthesis of $CaSnO_3$ nanorods/Bi_2WO_6 nanosheets composite

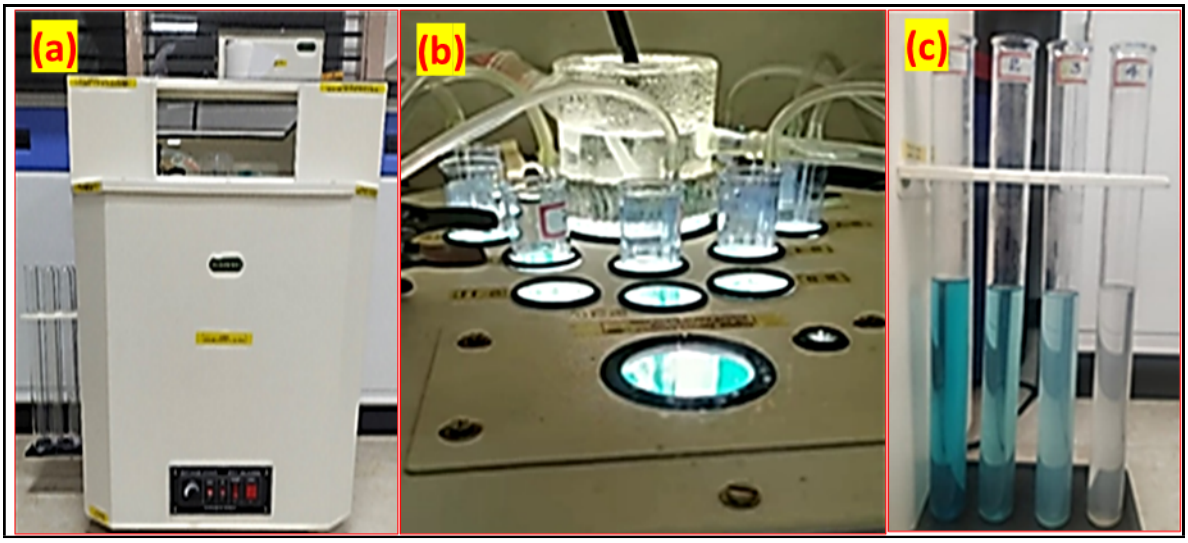

Fig. S2. (a) Represents the photocatalytic instrument, (b)Top view of the instrument during the photocatalysis and (c) Tubes contains reaction mixture after successive photodegradation.

Raman Studies:

Fig. S3 depicts the Raman plot of $CaSnO_3$/ Bi_2WO_6 compound. The formation of the composite is confirmed by the presence of both $CaSnO_3$ and Bi_2WO_6 compounds' Raman active modes. The active Raman peaks of orthorhombic $CaSnO_3$ phase are represented by 183, 275, 356 and 570 cm^{-1}. The three major symmetric modes of B_{2g}, A_g and B_{1g} are defined by 183, 275 and 356 cm^{-1} peaks. Raman modes centered at 746, 806, 1040, 1120, 1250 and 1300 cm^{-1} confirmed the presence of Bi_2WO_6 antisymmetric and symmetric A_g modes of O-W-O terminals of stretching vibrations. The Raman mode located at 950 cm^{-1} is attributed to the W=O stretching bond.

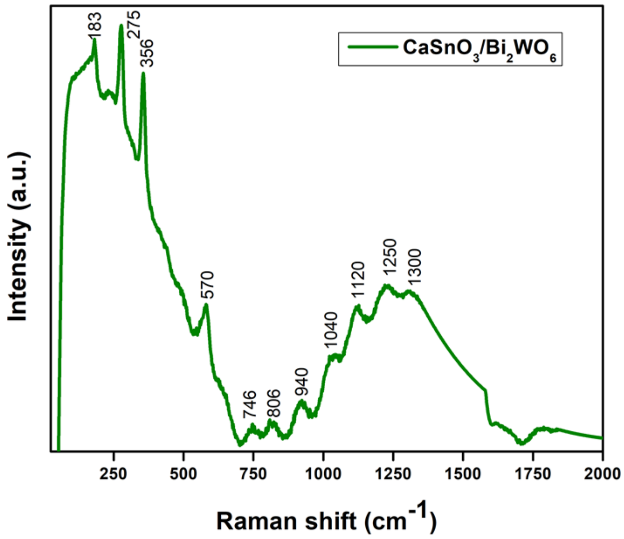

Fig. S3 Raman spectrum of $CaSnO_3/Bi_2WO_6$ compound

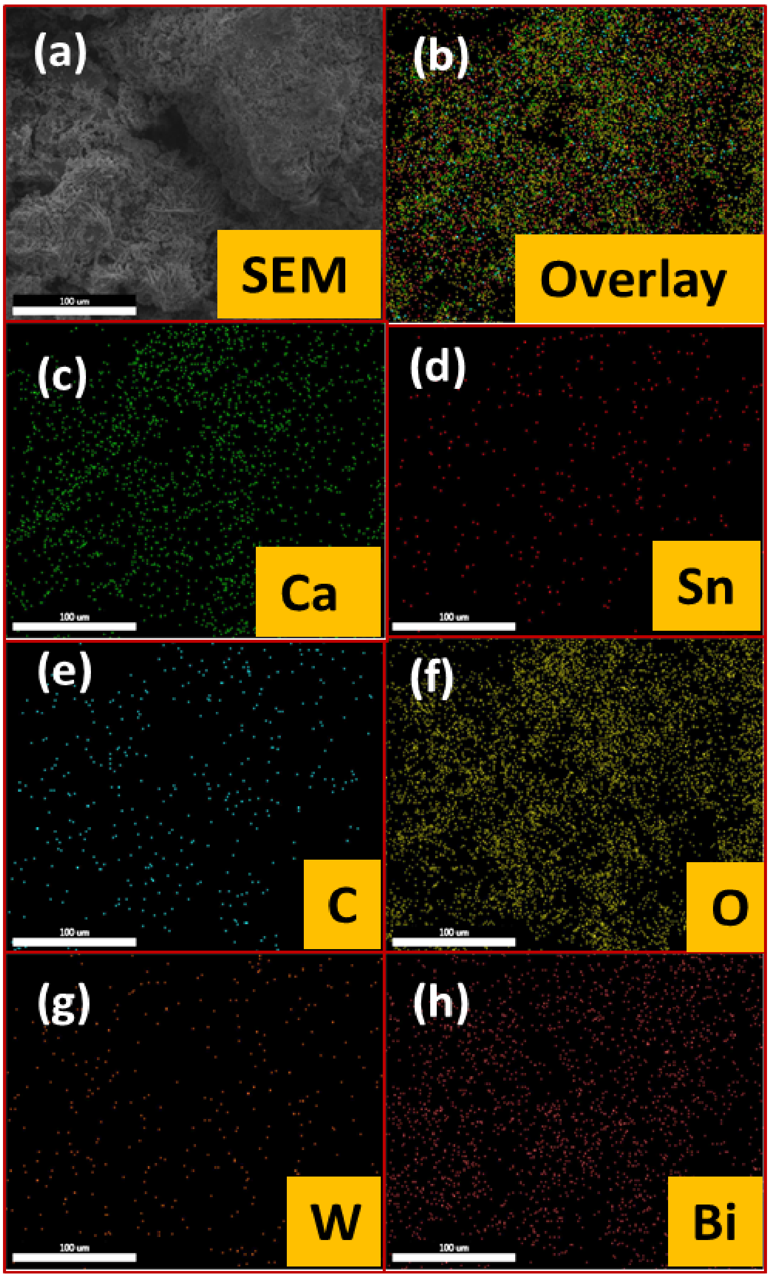

Fig. S4. Elemental mapping of $CaSnO_3/Bi_2WO_6$ composite material shows (a) SEM image, (b) Overlay image, (c) Calcium, (d) Tin, (e) Carbon, (f) Oxygen (g) Tungsten and (h) Bismuth

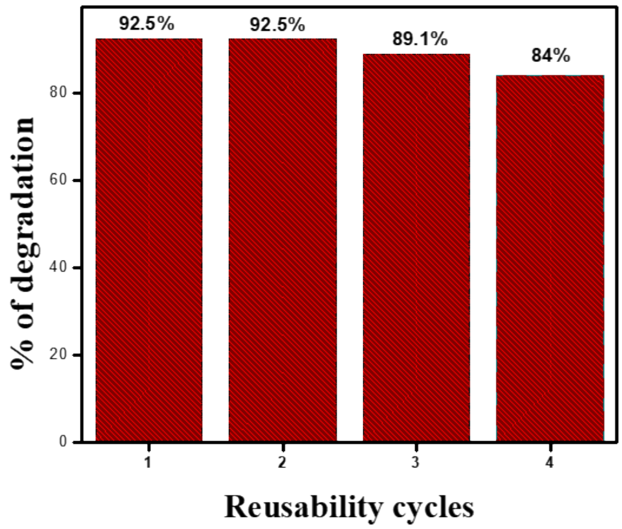

Fig. S5. Reusable ability graph of $CaSnO_3/Bi_2WO_6$ nanocomposite

Effect of Scavengers on photocatalytic dye degradation:

To assess the primary contribution of photogenerated species to dye degradation and to forecast a potential photocatalytic mechanism. We have taken three different scavengers, namely, benzoquinone BQ (1mM), ammonium oxalate AO (1mM) and tert-butyl alcohol TBA (1mM), to trap the superoxide ion radical ($^{\cdot}O_2^-$), hole (h^+) and photogenerated hydroxyl radical (·OH), respectively. The breakdown efficiency of the dye is significantly decreased in **Fig. S6.**, by adding several scavengers. According to analysis, scavengers like BQ, AO, and TBA have MB degradation efficiencies of 70, 64, and 23%, respectively. This illustrates how h^+ and $^{\cdot}O_2^-$ affect the dye degradation when exposed to visible light. However, the addition of TBA scavenges the activity of ·OH, leading to a significant reduction in the photocatalytic activity, suggesting that ·OH and are the primary dynamic species in dye photodegradation.

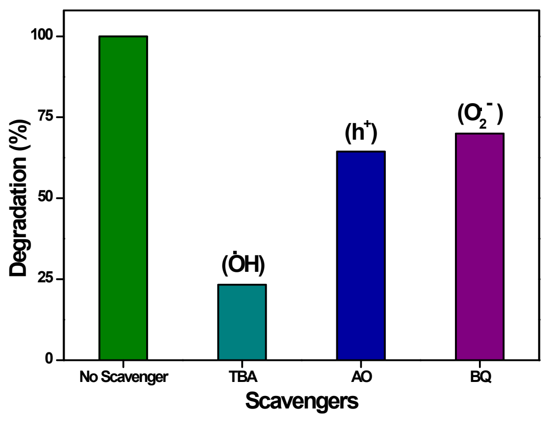

Fig. S6 Photocatalytic degradation for the kinetic studies of $CaSnO_3$/ Bi_2WO_6 composite

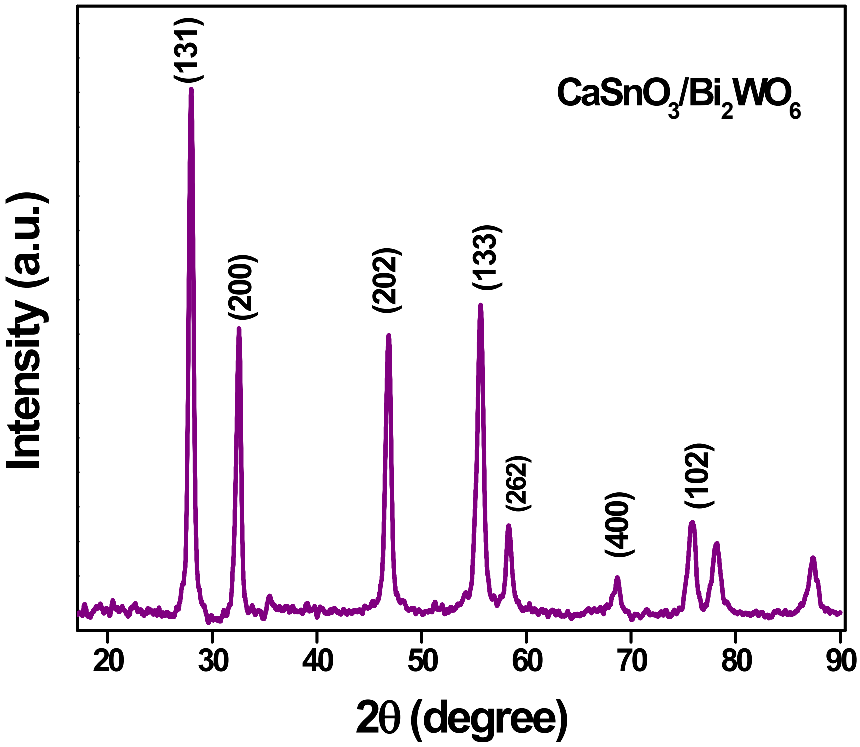

Fig. S7. XRD Pattern of $CaSnO_3/Bi_2WO_6$ nanocomposites after the degradation.

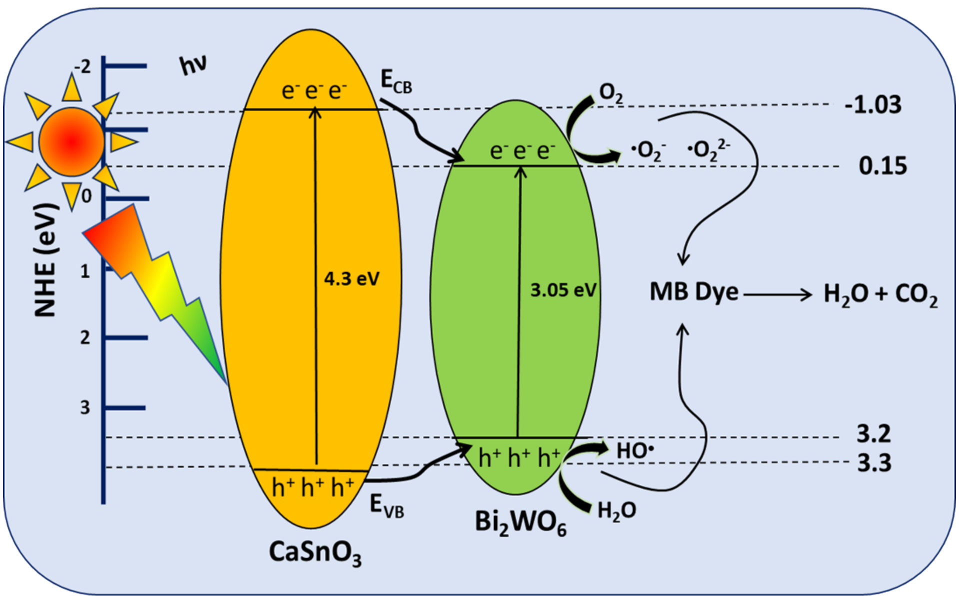

Fig. S8. Schematic representation of Type-I schemes for the photocatalytic MB degradation

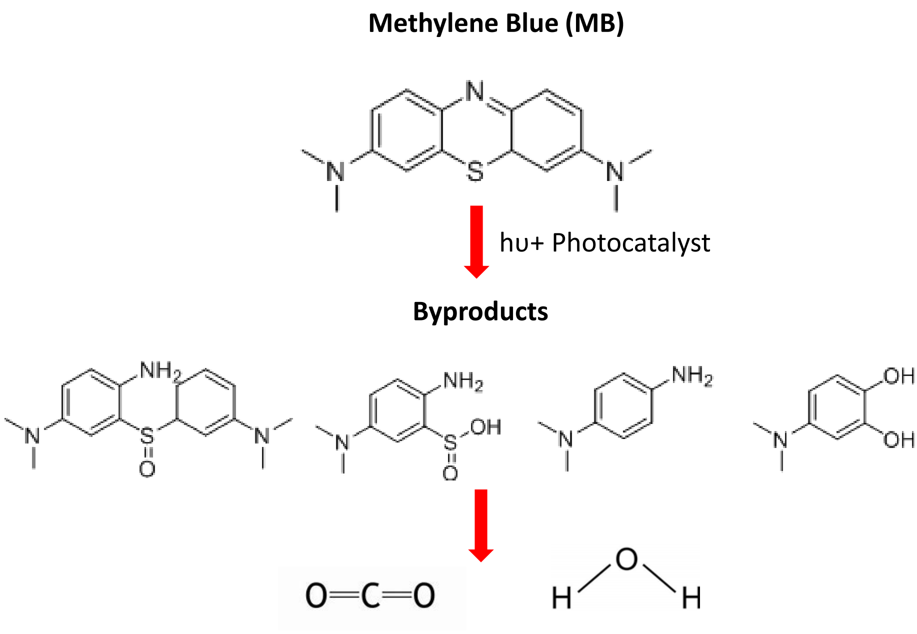

Fig. S9 Trajectory of photocatalytic degradation of Methylene blue

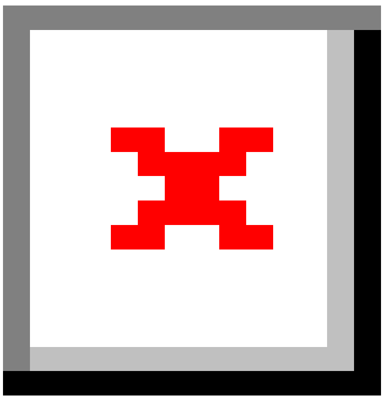

Fig. S9a. List of degradation intermediate structures with molecular weights

MS Spectrum

Line#:1 R.Time:----(Scan#:----)
MassPeaks:169
Spectrum Mode:Averaged 0.670-0.763(403-459) Base Peak:306(2762)
BG Mode:Averaged 0.000-0.663(1-399) Segment 1 - Event 1

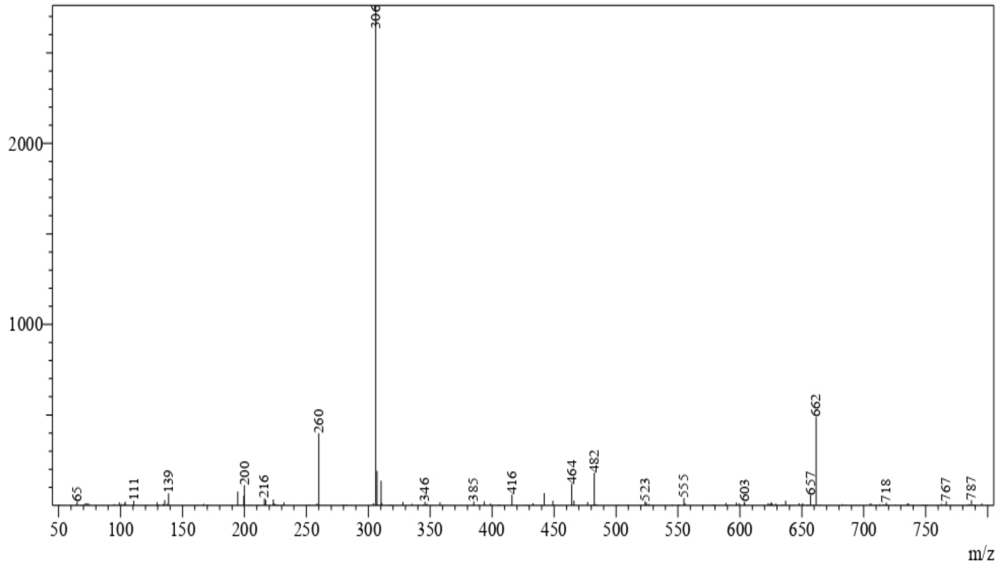

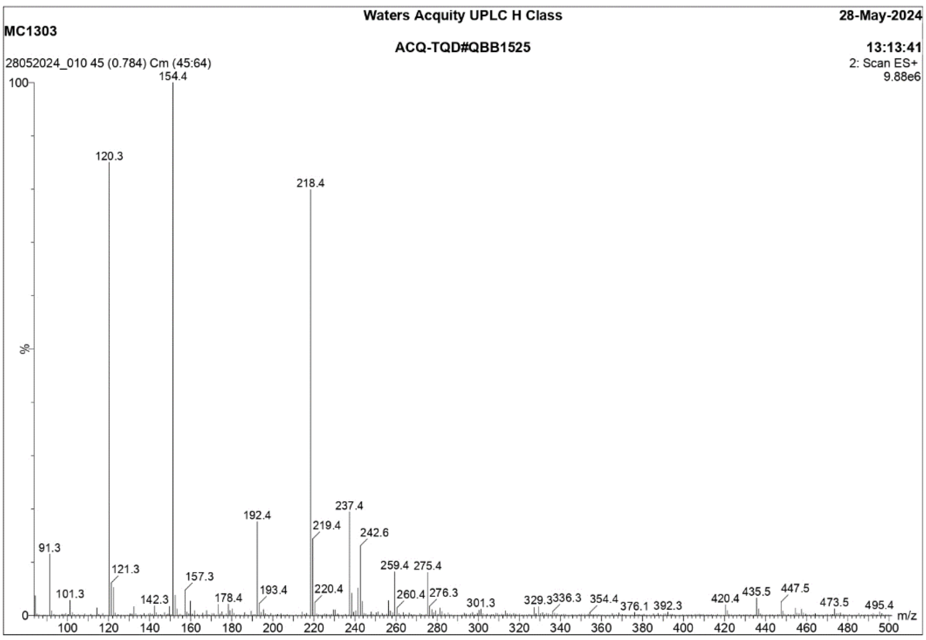

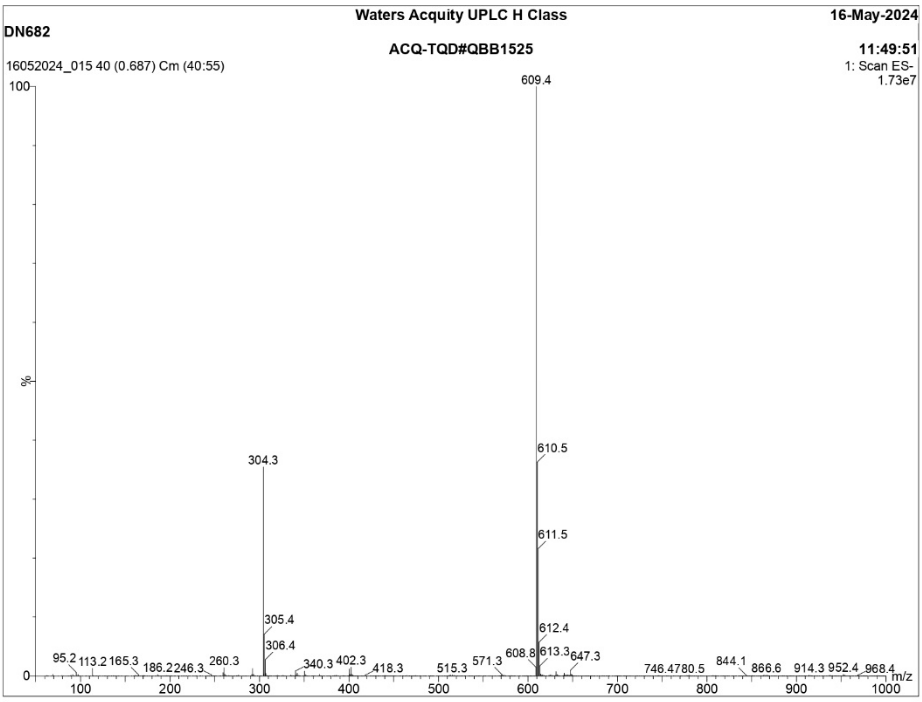

Fig. S9b. Mass spectrum of Methylene blue dye degradation intermediate products

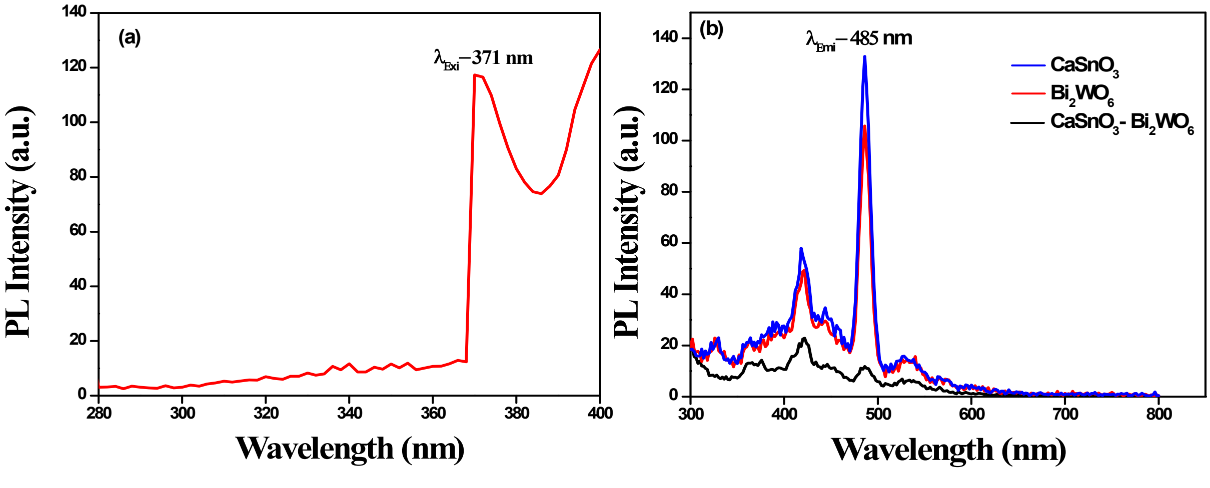

Fig. S10. Photoluminescence spectra of **(a)** Excitation spectrum, **(b)** Emission plots of $CaSnO_3$, Bi_2WO_6, $CaSnO_3/Bi_2WO_6$

Effect of CV with different pH:

The cyclic voltammogram of the modified GCE compound with $CaSnO_3/Bi_2WO_6$ at various pH values is shown in **Fig. S11**. The oxidation peak current response is observed within 50 µA in the electrocatalytic activity of the elementary weak alkali (pH 9) and strong acidic (pH 4). The oxidation current response for the slightly acidic pH 6 increased to 80 µA; for the neutral pH 7, it reached a higher value of 165 µA. This reveals that pH variation does not impact sensing for the $CaSnO_3/Bi_2WO_6$ modified GCE.

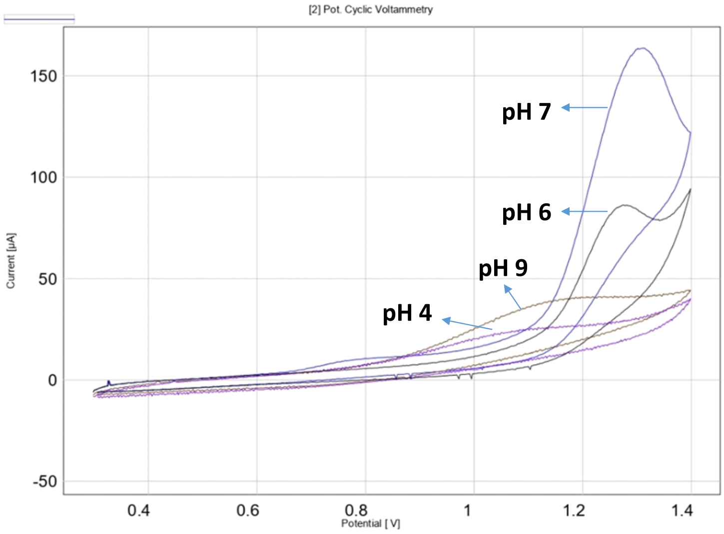

Fig. S11 Cyclic voltammogram of $CaSnO_3/Bi_2WO_6$ compound at different pH values

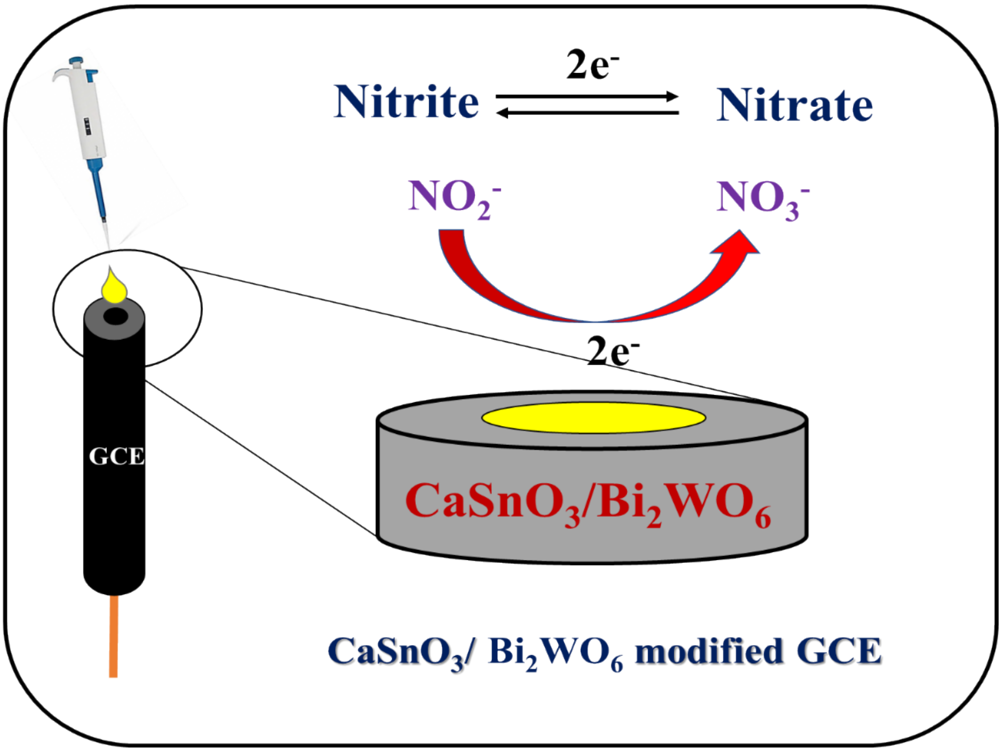

Fig. S12. Schematic representation showing the mechanism of electrochemical nitrite sensing by $CaSnO_3/Bi_2WO_6$ modified glassy carbon electrode